



Design of Genetic Algorithm Based Robust LQG Controller for Active Magnetic Bearing System

Enderias Alemayehu Workeye^{1(✉)}, Tamiru Getahun G/Meskel¹,
and Yakob Kiros T/Himantot²

¹ Adama Science and Technology University, Adama, Ethiopia

² Ethiopian Institute of Technology-Mekelle, Mekelle University,
Mekelle, Ethiopia

Abstract. The Active Magnetic Bearing system (AMB) is a mechatronic device which is used to suspend rotating parts of a machine so that they rotate without contact to the stationary part of the machine. AMBs are highly non-linear, non-minimum phase and inherently unstable. This paper has aimed to obtain a robust optimal state-feedback control system for the stabilization of the AMB System, with the help of Genetic algorithm (GA) as an optimization tool which will solve the tedious manual tuning of the weighting matrices in the design of linear quadratic regulator (LQR) and linear quadratic Gaussian (LQG).

The system's mathematical model has been developed and also the properties of the uncontrolled system have been analyzed. Since AMB is a MIMO system, the interaction of the inputs with the outputs has been analyzed using relative gain array analysis and frequency domain analysis of the system transfer functions. Then, the optimal state feedback controllers have been developed. Here, LQR and LQG controllers are developed.

Finally, Comparative analysis between the controllers and between the design methods was carried out. The proposed GA based design methodology has resulted good Performance. In addition, the GA based design has also resulted improvements in robustness of the control systems. As far as gain margin (GM) and phase margin (PM) are concerned GA has resulted increase of $8.0 \cdot 10^{-4}$ db and $6.02 \cdot 10^{-3}^\circ$ in GM and PM respectively for LQR. Whereas, in LQG GA has resulted an increase of $3.8 \cdot 10^{-5}$ db and $2.54 \cdot 10^{-4}^\circ$.

Keywords: Active magnetic bearing · Genetic algorithm · Linear quadratic Gaussian · Kalman filter

1 Introduction

Bearings are machine elements of a mechanism. They constrain the relative motion of a certain mechanical structure only to the desired motion, and reduce friction between moving and stationary parts.

There are many types of bearings which differ based on their operation, the motions allowed, or the directions of the loads (forces) applied to the parts. Despite the diverse types, Ball bearings are the oldest and most common types [1]. Ball bearings use balls

to maintain separation between the bearing races. Mostly they have two races to contain the balls and transfer the load forces through the balls.

Most electrical machines and wheels use ball bearings. In such applications, one race is stationary and the other is attached to the rotating machine part (e.g., a rotor or shaft). As one of the bearing races rotates it causes the balls to rotate as well, as a result the coefficient of friction will be reduced compared to two flat surfaces sliding against each other.

In Magnetic Bearings (MBs), the balls between the two races are replaced by a magnetic field. One of the two races will be suspended/levitated by a magnetic force. Such mechanisms provide all the functions of the ball bearings and since there is no physical contact, the friction will be almost zero. The magnetic field used to maintain the separation between the two races can be supplied either by permanent magnets or electromagnets.

Implementing magnetic bearings using permanent magnets requires intense design effort, the highest quality (almost ideal) of materials and gives no possibility to actively control the system in order to dump disturbances [3]. Due to this most magnetic bearings are powered by electromagnets.

Active magnetic bearings (AMBs) are mechatronic systems that support a rotating shaft with a magnetic field generated by electromagnets controlled in feedback. The rotor is levitated in an air gap. As shown in Fig. 1, using the feedback loop the performance is actively controlled. In the name of the AMBs the term active represents the continuous and active control action required in order to make the system functional and the use of electric power to energize the levitation.

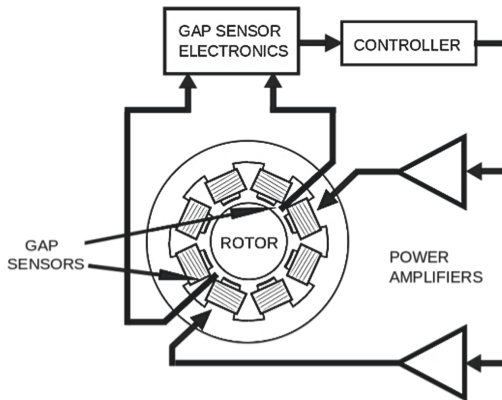


Fig. 1. The AMB control system [3].

2 Active Magnetic Bearings

AMBs are applied for enhancing the speed and efficiency of electrical machines. Therefore, they are used to suspend the rotor at a fixed air gap from the stator so that it rotates without any contact.

The AMB system considered in this paper has four electromagnetic actuators, as shown in Fig. 1, on both ends of the rotor. In reference to the horizontal axis the current

in the upper half electromagnetic actuators produce a magnetic force which counteracts the force of gravity and enables the ferromagnetic rotor shaft to levitate. Whereas current in the lower half electromagnetic actuators produce a magnetic force which acts along with gravity to make sure the magnetic force by the upper actuators does not cause unnecessary upward displacement [2].

T. Schuhmann, et al. (2012), has proposed “Improving Operational Performance of Active Magnetic Bearings Using Kalman Filter and State Feedback Control,” [6]. In this paper, the application of optimal state estimation using extended Kalman filter and optimal state feedback algorithms (LQG) for real-time active magnetic bearing control is considered. It is shown that this controller yields improved rotor positioning accuracy, better system dynamics, higher bearing stiffness, and reduced control energy effort compared to the conventionally used proportional-integral-derivative (PID) control approaches. In addition, a method for compensating unbalance caused by forces and vibrations of the magnetically levitated rotor is presented which is based on the estimation of unknown disturbance forces. In this paper a methodology on how to tackle the optimization problem along with noise compensation has been presented; however, the robustness of the controller designed has not been addressed and the design approach of the LQG was based on the trial and error tuning of the weighting matrices.

İ. Sina Kuseyri, in his paper titled “Robust control and unbalance compensation of rotor/active magnetic bearing systems”, [7] has designed, analyzed and compared the performance of various stabilizing robust controllers for the model of a horizontal rotor with active magnetic bearings. Two H^∞ controllers are designed for the nominal system using different structures. The uncertainties in the system dynamics due to changes in the model parameters are two-fold: gyroscopic forces due to different rotor speeds within the range of operation, and the changing spring stiffness of the electromagnetic bearings due to different conditions during the operation. To ensure robust stability of the closed-loop system for all possible values of parameters that can change during the operation, an H^∞ controller based on the model incorporating uncertainty in the system is designed. The limits for the allowable parameter changes for robust stability are tested and established with μ -analysis. The paper is highly focused on the stability and robustness of the system; however, it has not proposed about optimization of the control effort of the controller designed.

A paper titled “Active Magnetic Bearing Online Levitation Recovery through μ -Synthesis Robust Control” [8] by Alexander H. Pesch, et al. (2017), has presented in the event of momentary loss of levitation in Active magnetic bearings due to an acute exogenous disturbance or external fault, reestablishing levitation may be prevented by unbalance forces, contact forces, and the rotor’s dynamics. A novel robust control strategy is proposed for ensuring levitation recovery. The proposed strategy utilizes model-based μ -synthesis to find the requisite AMB control law with unique provisions to account for the contact forces and to prevent control effort saturation at the large deflections that occur during levitation failure. The proposed strategy is demonstrated experimentally with an AMB test rig and the proposed control strategy shows a marked improvement in re-levitation transients. However, the μ -synthesized controllers are high order [9]. For industrial implementation, further reduction of the weighted plant model or the synthesized controller may be required; therefore, practical implementation is not going to be feasible.

In this paper, Genetic Algorithm (GA) based Robust Linear Quadratic Gaussian (LQG) Controller that has good performance and robustness with minimum possible control effort for an Active Magnetic Bearing (AMB) system is designed, thus the AMB will levitate and maintain central position for the rotor despite the plant disturbance and measurement noises.

3 Problem Formulation

Active magnetic bearings have a significant advantage in increasing the efficiency of different machines. They practically avoid the loss due to frictional force, but the systems are highly nonlinear, non-minimum phase, and unstable system [2].

In the case of high speed rotating machines the rotor must be regulated in the desired position for smooth operation. Beside the nonlinearity and un-stability, the model uncertainty and neglecting of some higher frequency dynamics due to simplification for computation may make the system unrealistic when implemented in real system, therefore robustness is another problem.

It is possible to overcome the above mentioned properties of the AMB with the design of controller with a very high control effort in order to guarantee robustness. But still, the control effort should be as minimum as possible. Therefore, here optimization comes in to the picture. Furthermore, the controller designed should be realizable and lower order. Since, higher order control systems are quite difficult and costly to implement.

The control of AMB systems mostly has not tried to solve the Robustness and optimization problems fully at once. Therefore, this will not give the full picture on the performance and appropriateness the controller for the AMB system.

In addition, in the design of optimal state feedback controllers like LQR and LQG, the selection of the values of the weighting matrices Q and R is done by trial and error. This is done by setting them on some value and observing the performance of the closed loop step response. Such methodology is tedious and time consuming.

Therefore, observer based state feedback controllers (LQGs) are designed to stabilize the system with optimal control effort. In the design of the LQG the selection of the weighting matrices has been under taken by using the genetic algorithm (GA). In addition, the robustness of the control systems will be analyzed.

4 Mathematical Model of Amb

The active magnetic bearing system has (AMB) has three main system components.

The power amplifier, electro-magnetic actuator and the rotor as illustrated in Fig. 2 below.

The block diagram of AMB control system. The plant consists of power amplifier, AMB actuator and the rotor mass system. Vectors r , u , i , f and y represent the reference input, plant input (control current), coil current, magnetic force, and plant output (rotor displacement), respectively. In addition, the additive measurement noise is represented by v .

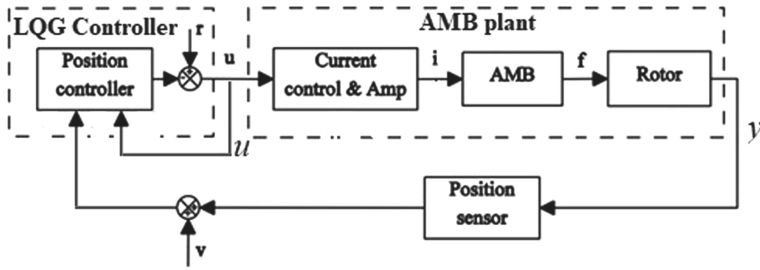


Fig. 2. The Block diagram of the AMB control system

4.1 Modeling of the AMB Actuator

The electromagnetic actuators in Active Magnetic Bearings accept current signal from the power amplifiers and then the flow of current via the coils generates a magnetic force. The AMBs considered in this paper are two sided bearings. In two sided bearings the upper bearings are used to overcome the weight of the rotor due to gravity and suspend it. The fixed current required by the upper bearing to overcome the weight of the rotor due to gravity is determined by the non-linear equation of electromagnetic force given below.

$$f = \frac{k * i^2}{2x^2} \tag{1}$$

After the linearization of (1) at the equilibrium points (the biasing current ‘ i_0 ’ and the nominal air gap ‘ x_0 ’) the linear force equation is given by the following relation.

$$f = K_s x_x + K_i i_x \tag{2}$$

Where K_s and K_i are given by:

$$K_s = \frac{k * i_0^2}{2 * x_0^3} \quad \text{and} \quad K_i = \frac{k * i_0}{2 * x_0^2}$$

4.2 Modeling the Power Amplifiers

The amplifier model accepts the voltage signal from the controller and outputs the current signal to the actuator coil. It does so by employing a closed loop control of its own. The current control is usually a pure proportional control. Under the assumption that the coil resistance R_C is small and the inductance L is constant, the following transfer function in (3) is obtained [5].

$$G_a(s) = \frac{Kp}{sL + (Kp + Rc)} = \frac{Kp}{sL + Kp} \tag{3}$$

Where, KP is the proportional gain of the amplifier. KP is highly dependent on the band-width of the amplifier denoted by ω_{bw} .

$$Ga(s) = \frac{(\omega_{bw})}{(s + \omega_{bw})} \tag{4}$$

Where,

$$\omega_{bw} = \frac{Kp}{L} \tag{5}$$

In order to determine the bandwidth of the power amplifier,

$$\omega_{bw} = \frac{\text{Cos}(\alpha) * P_{max}}{X_0 * F_{max}} \tag{6}$$

Where, α is the angle between consecutive poles of the electromagnetic actuators and P_{max} and F_{max} are the maximum power by the amplifier and the maximum force required by the actuator respectively.

$$F_{max} = K_i * i_{max} + K_s * X_{max} \tag{7}$$

$$i_{max} = 2 * i_0 \text{ and } X_{max} = 2 * X_0 \tag{8}$$

Using the state space representation, the model of the amplifier will be:

$$\frac{d}{dt} \begin{vmatrix} i_A \\ i_B \end{vmatrix} = \begin{vmatrix} -\omega_{bw} & 0 \\ 0 & -\omega_{bw} \end{vmatrix} \begin{vmatrix} i_A \\ i_B \end{vmatrix} + \begin{vmatrix} \omega_{bw} & 0 \\ 0 & \omega_{bw} \end{vmatrix} \begin{vmatrix} u_A \\ u_B \end{vmatrix} \tag{9}$$

4.3 Modeling the Rigid Rotor

The rotor mass system is supported with two radial AMBs. As shown in Fig. 3 the axial support is not considered here. This is justified by the negligible coupling of the axial and radial dynamics.

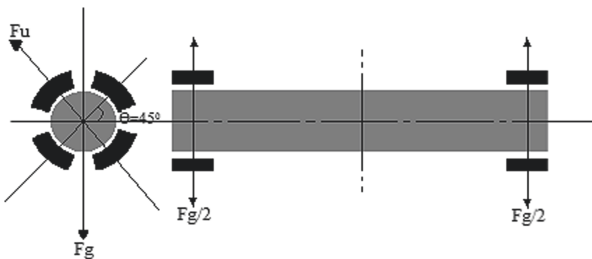


Fig. 3. Sectional view for the rotor mass-bearing system

Moreover, this analysis is restricted to rigid rotors at stand still. Such approach is taken to avoid the coupling that occurs between radial motions in the two perpendicular planes. As a result, it is possible to analyze the motion in one plane.

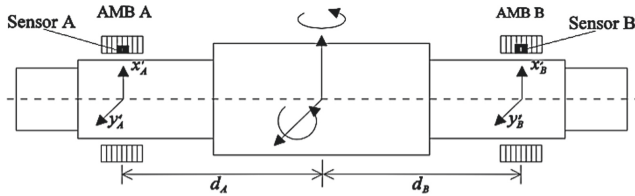


Fig. 4. Cross-sectional view of the AMB-rotor assembly [2].

The radial motion in one plane can be completely described by a rigid beam model, i.e. by the displacement X of the rotor and the rotation of the rotor about an axis through the center of gravity as shown in Fig. 4.

The forces and displacement that put effect on the rotor are resolved along the X and Y planes. Bearings A and B are separated from the center of gravity of the rotor by d_A and d_B respectively.

The mathematical model of the rotor mass system is done by integrating it with the electromagnetic actuator model. Therefore, the force balance equation of the actuator-rotor system is given as:

$$M * \ddot{X} = f \tag{10}$$

$$M * \ddot{X} = K_s x + K_i i \tag{11}$$

$$\ddot{X} = M^{-1} K_s x + M^{-1} K_i i$$

Where, M is the mass matrix of the rotor given as:

$$M = \begin{vmatrix} m_1 & m_3 \\ m_3 & m_2 \end{vmatrix} \tag{12}$$

And m_1 , m_2 and m_3 are given by;

$$m_1 = \frac{M * d_B^2 + I_r}{(d_A + d_B)^2} \tag{13}$$

$$m_2 = \frac{M * d_A^2 + I_r}{(d_A + d_B)^2} \tag{14}$$

$$m_3 = \frac{M * d_A * d_B - I_r}{(d_A + d_B)^2} \tag{15}$$

I_r represents the radial moment of inertia of the rotor. In this paper, the center of gravity of the rotor is assumed to be at the center of the axial length of the rotor. As a result, ‘ d_A ’ and ‘ d_B ’ will have equal length.

The Non-linear model is based on the non-linear force equation given in (1).

$$\begin{vmatrix} \ddot{X}_A \\ \ddot{X}_B \end{vmatrix} = \begin{vmatrix} f(X_A, i_A) \\ f(X_B, i_B) \end{vmatrix} * M^{-1} \tag{16}$$

From Eq. (1) we can write $f(X_A, i_A)$ and $f(X_B, i_B)$ as follows:

$$f(X_A, i_A) = k \frac{i_A^2}{X_A^2} \tag{17}$$

$$f(X_B, i_B) = k \frac{i_B^2}{X_B^2} \tag{18}$$

Then Eq. (16) becomes (Table 1);

$$\begin{aligned} \ddot{X}_A &= \left(\frac{m_2}{m_1 * m_2 - m_3^2} \right) * k \frac{i_A^2}{X_A^2} - \left(\frac{m_3}{m_1 * m_2 - m_3^2} \right) * k \frac{i_B^2}{X_B^2} \\ \ddot{X}_B &= \left(\frac{-m_3}{m_1 * m_2 - m_3^2} \right) * k \frac{i_A^2}{X_A^2} + \left(\frac{m_1}{m_1 * m_2 - m_3^2} \right) * k \frac{i_B^2}{X_B^2} \end{aligned}$$

Table 1. AMB parameter values

No	Parameter	Symbol	Value [Unit]
1	Mass of Rotor	M	$1.39 * 10^1$ [Kg]
2	Moment of inertia	I_x	$1.34 * 10^{-2}$ [Kg.m ²]
3	Rotor length	L	$2.6 * 10^{-1}$ [m]
4	Permeability of free space	μ_0	$4\pi * 10^{-7}$ [H/m]
5	Number of coil	n_c	269 [turns]
6	Area of coil	A_c	$5.7375 * 10^{-4}$ [m ²]
7	Steady air gap	x_0	$3 * 10^{-3}$ [m]
8	Biasing current	i_0	3 [A]
9	Number of poles	p	8 [number]
10	Power Amplifier BW	ω_{bw}	300 [Hz]

Finally, the overall model of the AMB system is obtained by combining all state equations of the sub-systems. Therefore, using the state space representations obtained on (9) and (16) we obtain the overall system state space representation.

$$\frac{d}{dt} \begin{pmatrix} i_A \\ i_B \\ X_A \\ X_B \\ \dot{X}_A \\ \dot{X}_B \end{pmatrix} = \begin{pmatrix} -300 & 0 & 0 & 0 & 0 & 0 \\ 0 & -300 & 0 & 0 & 0 & 0 \\ 0 & 0 & 0 & 0 & 1 & 0 \\ 0 & 0 & 0 & 0 & 0 & 1 \\ 10.7206 & -9.5648 & 10.7206 & -9.5648 & 0 & 0 \\ -9.5648 & 10.7206 & -9.5648 & 10.7206 & 0 & 0 \end{pmatrix} \begin{pmatrix} i_A \\ i_B \\ X_A \\ X_B \\ \dot{X}_A \\ \dot{X}_B \end{pmatrix} + \begin{pmatrix} 300 & 0 \\ 0 & 300 \\ 0 & 0 \\ 0 & 0 \\ 0 & 0 \\ 0 & 0 \end{pmatrix} \begin{pmatrix} u_A \\ u_B \end{pmatrix}$$

$$Y = \begin{pmatrix} 0 & 0 & 1 & 0 & 0 & 0 \\ 0 & 0 & 0 & 1 & 0 & 0 \end{pmatrix} \begin{pmatrix} i_A \\ i_B \\ X_A \\ X_B \\ \dot{X}_A \\ \dot{X}_B \end{pmatrix} + \begin{pmatrix} 0 & 0 \\ 0 & 0 \end{pmatrix} \begin{pmatrix} u_A \\ u_B \end{pmatrix}$$

The Active magnetic bearing represented by the above state-space model has right hand side poles and zeroes which will make the system to be unstable and non-minimum phase.

5 Interaction and Coupling

One of the most challenging aspects of MIMO systems control is the interaction between different inputs and outputs. In the AMB control system the control action on bearing A not only affects the position of the rotor at bearing A but, it will also have effect on the position of the rotor at bearing B and the vice-versa.

A certain MIMO system is totally decoupled when the non-diagonal elements of the square transfer matrix functions are zero. In other words, if the transfer matrix is a diagonal matrix the system is said to be decoupled [14].

The RGA will show the measure of process interaction and gives indication of control loop pairings [14].

$$\Lambda(G) = G(0) \cdot G^{-T}(0) \tag{19}$$

For the AMB system with transfer matrix the RGA is calculated as:

$$\Lambda(G) = \begin{bmatrix} \lambda_{11} & \lambda_{12} \\ \lambda_{21} & \lambda_{22} \end{bmatrix} = \begin{bmatrix} \lambda_{11} & 1 - \lambda_{11} \\ 1 - \lambda_{11} & \lambda_{11} \end{bmatrix} \tag{20}$$

Therefore, the relative gain array (RGA) will be:

$$\Lambda(G) = \begin{bmatrix} 1 & 0 \\ 0 & 1 \end{bmatrix} \tag{21}$$

From the RGA result obtained above $\lambda_{11} = \lambda_{22} = 1$ indicates that coupled interaction does not affect the pairing of U1 with Y1 and U2 with Y2. Therefore, it is a clear that we should select the two loops since we can sufficiently manipulate the outputs Y1 and Y2 using the input control signals U1 and U2 respectively.

6 Controller Design

The controllers designed for AMBs supply the electro-magnetic actuators the appropriate control signal to maintain the rotor at the desired central position.

6.1 LQR Design

Linear quadratic regulators as the name indicates, they are linear state feedback controllers. The LQR is the extension of pole placement technique that tends to find the control input $u(t)$ so as to place the poles of the system at a desired optimal position. This is done by minimizing a quadratic cost function J given below.

$$J = \frac{1}{2} \int_{t_0}^{t_f} [x^T(t)Q(t)x(t) + u^T(t)R(t)u(t)]dt \quad (22)$$

And the control input $u(t)$ is given as:

$$u(t) = r - K * x(t) \quad (23)$$

The cost function is the time integral of the sum of the transient energy and control energy. The LQR should minimize this cost function while obtaining the state feedback gains K that drives the system to the desired operating point.

$$K = R^{-1}B^T P \quad (24)$$

The optimal state feedback control gain matrix K of LQR can be found by solving the following arithmetic Riccati equation.

$$A^T P + PA + Q - PBR^{-1}B^T P = 0 \quad (25)$$

Where, P is the solution of the Arithmetic Riccati equation.

The selection of the weighting matrices Q and R for the LQR design is done by; first keeping the R matrix constant ($R = \text{diag}([1, 1])$) and checking for different Q values.

Q matrix values are going to be selected based on the performance of the LQR. Therefore, Q values are kept constant at 0.01 and LQR is designed for different R matrix values.

It can be observed that the rise time, settling time, steady state error and peak responses are improved as magnitude of the values of R matrix increases. Thus, it can be observed that the best result out of the four cases is obtained at $R_i = 10$.

This method is burdensome, time consuming and difficult to know whether it results in optimum performance or not. In order to address this problem, here it has been proposed genetic algorithm (GA) based optimization for selecting the weight matrices of LQR based on the time domain specifications of the system to be controlled.

Genetic algorithm (GA) is an intelligent optimization technique developed by John Holland. It is based on the principles of natural selection and genetic modification. The evolutionary theory attributes the process of the natural evolution of populations to Darwin's principle of natural selection, "survival of the fittest," and Mendel's genetics law of transfer of the hereditary factors from parents to descendants [10].

Compared with the traditional (enumeration, heuristic, etc.) genetic algorithm, optimization method has very good convergence. It has the advantages of less computing time, higher robustness in the calculating accuracy. So this paper uses constrained genetic algorithm, to search the optimal value of Q and R. The weighting matrices are generally used in the form of a diagonal matrix. For the Active magnetic bearing system, the parameters Q and R are optimized by using the following representation.

$$Q = \text{diag}(q_1, q_2, q_3, q_4, q_5, q_6) \quad \text{and} \quad R = \text{diag}(q_7, q_8)$$

The need for using constrained GA is that sometimes the work of basic genetic algorithm cannot solve the problem of large amount of calculation very well, the optimization result could produce results away from the actual or desired result.

The step in genetic algorithm optimization begins by creating a random initial population. The algorithm then creates a new generation or population using the individuals of the current population. To create new generation, the algorithm performs crossover and mutation in between the individuals of the current generation. Then the current generation is replaced by the children of the next generation. The children of the next generation are chosen on the basis of their best fitness value. The algorithm stops when one of the stopping criteria is met.

Genetic algorithm can be implemented in different ways. One can implement the algorithm by coding it in any desirable programming language. In the case of this paper, the MATLAB™ optimization toolbox has been used to implement the algorithm.

To implement the GA optimization, first the fitness function must be defined. The fitness function is the objective function that needs to be minimized. In this case the objective function contains the cost function J defined in (21) and also contains a function that represents the ISE (integral square of error) of the response of the system to a unit step input. Beside the fitness function the number of variables to be optimized should also be specified. The variables to be optimized are the diagonal elements of the Q and R matrices (Fig. 5).

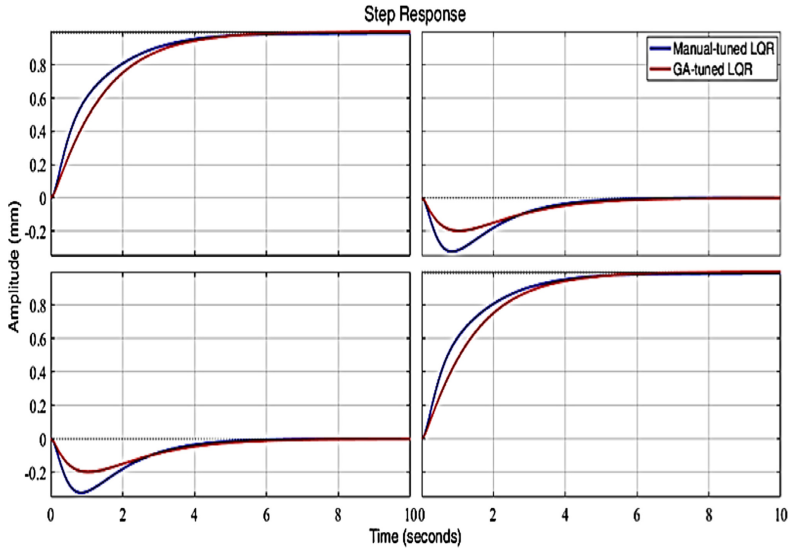


Fig. 5. Unit step response of GA-tuned LQR vs. Manually-tuned LQR

For the highly interacting input-output pairs, it can be observed that the performance of GA-tuned LQR is slightly degraded. The manually tuned LQR has a better response. The rise time and settling time of the GA-tuned LQR have shown slight increase compared to the manually-tuned LQR even though the result obtained satisfies the control objective.

Whereas, for the loosely interacting I/O pairs the GA-tuned LQR has managed to reduce the undershoot caused by input 1 on output 2 and input 2 on output 1 by 64.54%. This shows that the GA-tuned has reduced the unwanted effect of the inputs on the outputs in a significant manner.

Generally Linear Quadratic Regulators are designed for systems having a perfectly known model and also if all states of the system are available for measurement. In the case of Active magnetic bearings, the model of the system has its own level of uncertainty. This is due to the rejected model components during the linearization process. In addition, employing measurement techniques and devices to extract measurement of each and every state makes the control system quite expensive. Thus, this problem can be addressed by another controller design approach known as the Linear Quadratic Gaussian (LQG) Regulator.

6.2 LQG Design

Linear quadratic Gaussian regulators are optimal observer (Kalman Filter) based optimal state feedback controllers (LQR). In the design of LQG, based on the separation principle; the state estimator and state feedback controller are designed independently.

In LQG the Kalman filter estimates the states of the system by taking the control signal and the output of the system. The estimation of the states is undertaken in the presence of both process disturbance (d) and measurement noises (n). The stochastic noises i.e. the disturbance and measurement noises are modeled as white Gaussian noise.

For this controller design problem, the state-space model of the system has the following form (Fig. 6).

$$\frac{d}{dt}X = A * X + B * U + V_d * d \tag{26}$$

$$Y = C * X + D * U + V_n * n \tag{27}$$

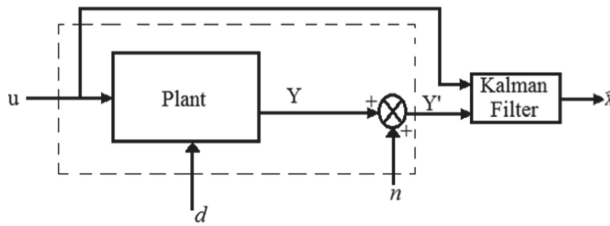


Fig. 6. State estimation using Kalman filter.

The kalman filter takes the control signal u and the plant output Y and gives out the estimate of the plant states. In Fig. 7 there are two parts, the augmented system with disturbance and noise, indicated by the dashed area and the Kalman filter.

Once the gains (L) of the Kalman filter are obtained, The KF will have the following state-space representation.

$$\frac{d}{dt}\hat{X} = (A - L * C)\hat{X} + [BL]U \tag{28}$$

$$Y' = eye(6)\hat{X} + 0 * [BL]U \tag{29}$$

The inputs of the Kalman filter are the control signals u and the plant outputs y.

$$U = [uv]^T$$

In order to inject the disturbances in to each state the augmented plant model can be developed as follows:

$$\frac{d}{dt}X = AX + [Bf]U \tag{30}$$

$$Y = eye(6)X + DU \tag{31}$$

Where, $[Bf]$ is an augment inputs to include disturbance and noise along with the plant input.

$$[Bf] = [BV_d0 * B]$$

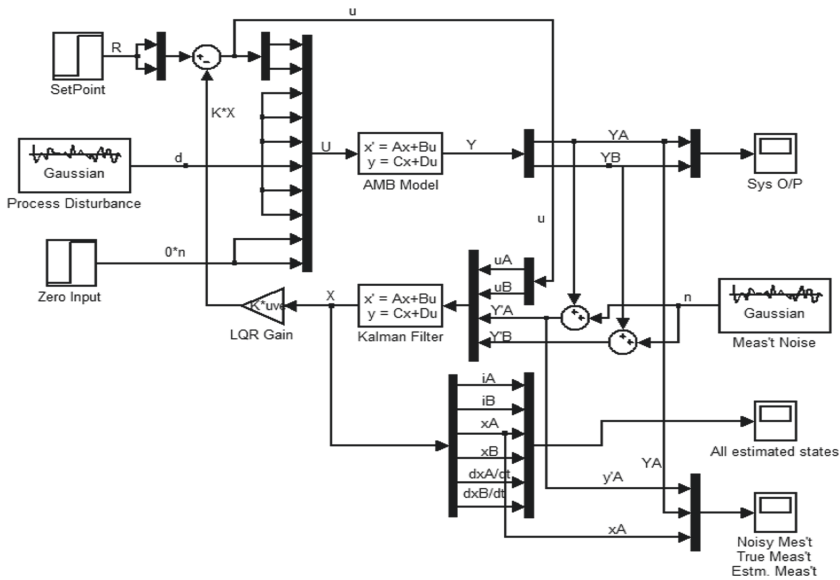


Fig. 7. The SIMULINK diagram of LQG for AMB

The performance of the Kalman filter designed has been evaluated in both noisy and less noisy conditions. The noisy condition the disturbance signal has a variance of 0.1. When the system is subjected to such process disturbances and measurement noises the Kalman filter was able to extract the output measurement out of the noise (Figs. 8 and 9).

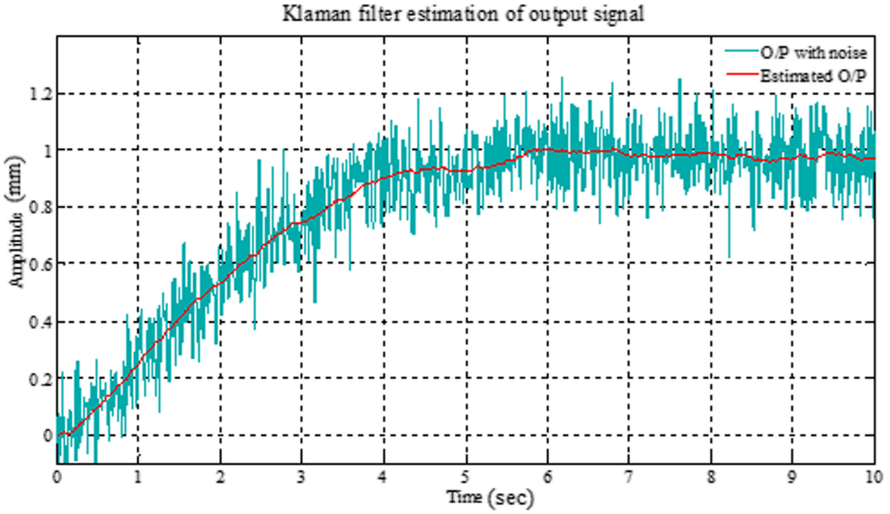


Fig. 8. Kalman filter estimation of the output signal out of the noisy measurement signal

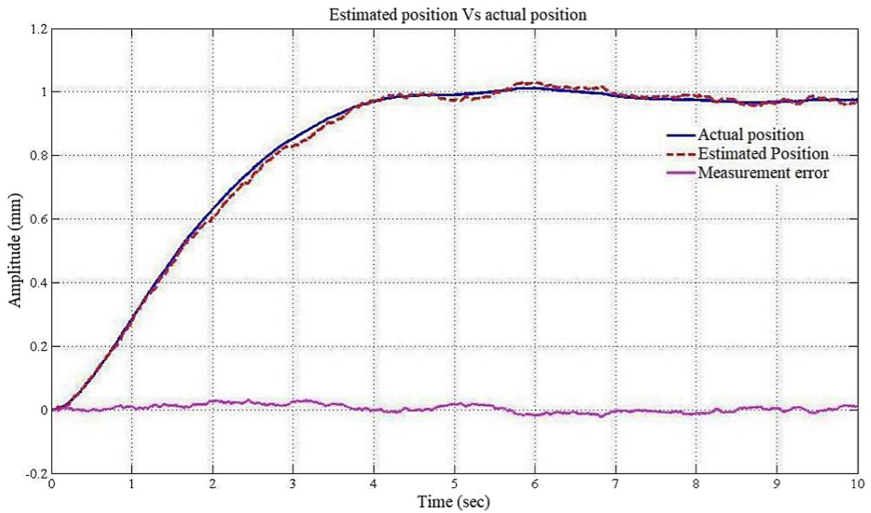


Fig. 9. Estimated state vs Actual state and estimation error in noisy condition

The performance of the LQG depends on how well the states are being estimated and on the performance of the LQR. The performance of the Kalman filter has already been established, and also in the LQR design the GA-based LQR was selected (Fig. 10).

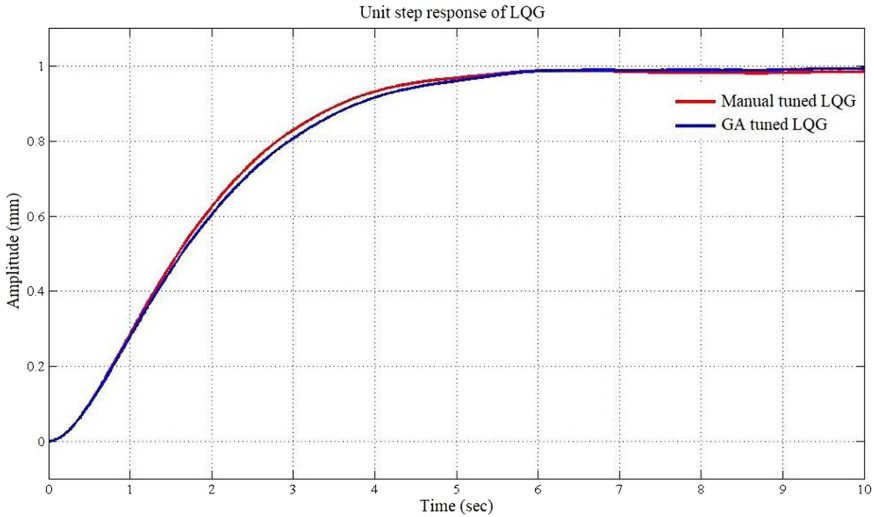


Fig. 10. Unit step response of GA-tuned LQG and manually tuned LQG

The GA-tuned LQG takes an advantage over not only by steady state performance but also the control effort required is also lower compared to manually tuned LQG (Table 2).

Table 2. Comparison of the performance of GA-tuned LQG and manually tuned LQG.

Specifications	GA-tuned LQG	Manual-tuned LQG
Settling time (t_s)	4.66 s	4.35 s
Rise time (t_r)	3.05 s	3.02 s
Steady state error (e_{ss})	0.006 mm	0.015 mm
Peak Response (Y_p)	0.994 mm	0.985 mm

7 Robustness Analysis

Robustness is the measure of how well the controller will perform if it is implemented in the actual AMB system. Prior to the analysis of robustness, the cases which may make the system to be not robust (model uncertainties) will be identified.

The model uncertainty in the AMB system can arise due to (Fig. 11):

1. Model parameter uncertainty
2. Neglected high frequency dynamics
3. Non-linearity
4. Changing operating conditions
5. Neglected dynamics
6. Setup variations

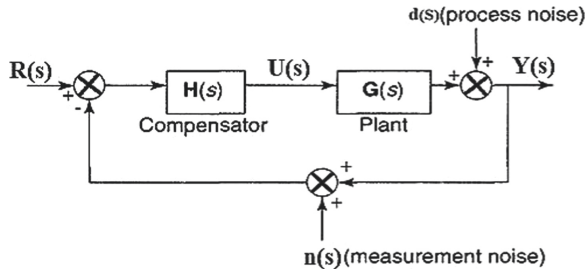


Fig. 11. A multivariable feedback control system with process and measurement noise

The sensitivity of the output of the system $Y(s)$ with respect to the process disturbance $d(s)$ and measurement noise $n(s)$ depend on the sensitivity function given by $[I + G(s)H(s)]^{-1}$. While the sensitivity of the input control signal $U(s)$ depends on the sensitivity function $[I + H(s)G(s)]^{-1}$.

In a certain closed loop system the larger the magnitude of the two sensitivity functions, the larger will be the sensitivity of the plant output and the input control signal to process disturbance $d(s)$ and measurement noise $n(s)$.

Return ratio matrix can be defined to analyze robustness. In order to simplify the measure of robustness, we can assign scalar measure of robustness than dealing with return difference matrix or return ration matrix. In order to accomplish this we can assign the scalar values (Singular Values) by defining matrix norm.

The most common way of identifying the singular values of a certain matrix is using singular value decomposition (SVD) algorithm. Singular values are very important to analyze property of multivariable feedback system. In the analysis of robustness the largest and smallest singular values of the return difference matrix as providing upper and lower bounds on the scalar return difference matrix.

7.1 Robustness at the Output

When we analyze robustness with respect to process disturbance $d(s)$ and measurement noise $n(s)$ independently, it has been summarized as follows:

- To maximize robustness with respect to process disturbance $d(s)$ $\delta_{\min}[G(s)H(s)]$ should be maximized
- To maximize robustness with respect to measurement noise $n(s)$ $\delta_{\max}[G(s)H(s)]$ should be minimized

The conditions stated in (a) and (b) conflict to each other. However, measurement noise usually has predominantly high frequency content. Therefore we can threat robustness for measurement noise and process disturbance in high frequency and low frequency respectively. Thus, it is compromised by minimizing δ_{\max} of $[G(s)H(s)]$ at high frequency and by maximizing δ_{\min} of $[G(s)H(s)]$ at low frequency.

Table 3. The singular values of $[G(j\omega)H(j\omega)]$ for different nominal frequencies.

Design methods	$\omega = 0.01$ rad/s		$\omega = 10$ rad/s		$\omega = 100$ rad/s	
	δ_{\min}	δ_{\max}	δ_{\min}	δ_{\max}	δ_{\min}	δ_{\max}
Manual LQR	1.9723	1.9843	0.1456	0.7189	0.0019	0.0138
GA-LQR	1.9801	1.9911	0.2056	0.7348	0.0023	0.0175
Manual LQG	0.6965	1.8533	0.1161	0.2221	$3.05 \cdot 10^{-8}$	$1.334 \cdot 10^{-7}$
GA-LQG	0.6754	1.8416	0.1184	0.2323	$3.14 \cdot 10^{-8}$	$1.778 \cdot 10^{-7}$

From the results given in Table 3 the output robustness the control systems with respect to the process disturbance can be compared. In the results, the one with largest δ_{\min} has a better robustness. Generally it can be observed that LQR has a better robustness compared to LQG. In fact this has been a well-established point by many scholars and in different journals [11].

The GA tuned LQR has the best robustness to process disturbance compared to the other three controllers. The manually tuned LQR has the next better robustness while manually tuned LQG and GA tuned LQG follow.

For output robustness with respect to measurement noise, the LQG controllers tend to have better measurement noise rejection. Thus, it must have the smallest δ_{\max} at higher frequency range. As it can be observed from the table the LQG controllers have very small values of δ_{\max} which shows that the LQG designed has better noise rejection capability compared to LQG. This is due to the ability of the Kalman filter being able to extract the states from a noisy measurement signal.

7.2 Robustness at the Input

The return difference matrix can be maximized which is maximizing the minimum singular value in the return difference matrix [12].

- The input robustness with respect to process noise or model uncertainty is improved if $\delta_{\min}[H(s)G(s)]$ is maximized.
- The input robustness with respect to measurement noise is improved if $\delta_{\min}[H(s)G(s)]$ is maximized (Table 4).

Table 4. The singular values of $[H(j\omega)G(j\omega)]$ for different nominal frequencies.

Design methods	$\omega = 0.01$ rad/s		$\omega = 10$ rad/s		$\omega = 100$ rad/s	
	δ_{\min}	δ_{\max}	δ_{\min}	δ_{\max}	δ_{\min}	δ_{\max}
Manual LQR	1.9723	1.9843	0.1456	0.7189	0.0019	0.0138
GA-LQR	1.9801	1.9911	0.2056	0.7348	0.0023	0.0175
Manual LQG	0.6965	1.8533	0.1161	0.2221	$3.05 \cdot 10^{-8}$	$1.334 \cdot 10^{-7}$
GA-LQG	0.6754	1.8416	0.1184	0.2323	$3.14 \cdot 10^{-8}$	$1.778 \cdot 10^{-7}$

For input robustness unlike to the output robustness, the GA tuned LQR and LQG have better robustness over the manually tuned LQR and LQG respectively. The Genetic algorithm based tuning of the weighting matrices Q and R has managed to improve the measurement noise rejection capability as far as the input control signal is concerned.

7.3 Gain Margin and Phase Margin

The singular values of the return difference matrix at the output in the frequency domain, $\delta[I + G(j\omega)H(j\omega)]$, can be used to estimate the gain and phase margins of a multivariable system [12]. By plotting singular value plots against frequency, for all frequencies, ω , in the frequency range of interest.

The gain and phase margins are defined using singular values, by taking the smallest singular value, δ_{\min} , of all the singular values of the return difference matrix at the output. Then a real constant, a , is determined, such that $\delta_{\min}[I + G(j\omega)H(j\omega)] > a$. Then the gain and phase margins are defined as follows [12]:

Figure 12 and Fig. 13 show the singular values of the return difference ratio of the AMB control systems. From the first figure it can be observed that the smallest singular value of manually tuned LQR reaches minimum of -40.6725 dB at frequency of 100 rad/s. The smallest singular value of the manually tuned LQG reaches minimum value -77.9141 dB at 100 rad/s.

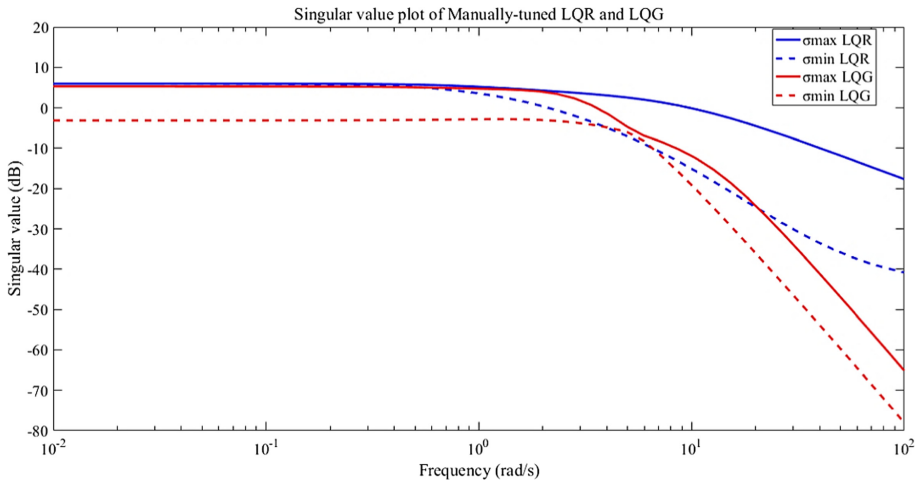


Fig. 12. Singular value plot of $[I + G(s)H(s)]$ of manually tuned LQR and LQG

Similarly as shown in the Fig. 13 the smallest singular value of GA-tuned LQR reaches a minimum of -40.722 dB at 0.01 rad/s. The GA-tuned LQG’s smallest singular values reach minimum of -77.7643 dB at 0.01 rad/s.

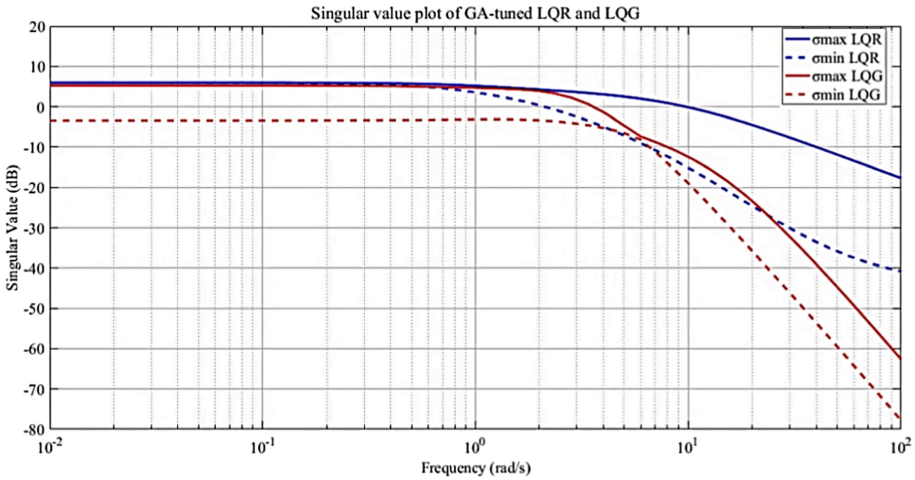


Fig. 13. Singular value plot of $[I + G(s)H(s)]$ of GA-tuned LQR and LQG

Table 5. The minimum and maximum gain and phase margins of the four controllers

Design methods	δ_{\min} (dB)	A	Gain margin (dB)	Phase margins (deg)
Manual LQR	-40.7220	0.009202	0.1606	1.05452
GA-LQR	-40.6725	0.009255	0.1614	1.06054
Manual LQG	-77.9141	1.2714×10^{-4}	0.002208	0.01457
GA-LQG	-77.7643	1.2935×10^{-4}	0.002246	0.014824

Observing the results from Table 5, the GM and PM of LQR obviously exceeds the GM and PM of LQG. On the other hand, concerning on the tuning methodologies, the GA tuning has relatively a better GM and PM in both LQR and LQG case compared to manual tuning. Observing the results from Table 5, the GM and PM of LQR obviously exceeds the GM and PM of LQG. On the other hand, concerning on the tuning methodologies, the GA tuning has relatively a better GM and PM in both LQR and LQG case compared to manual tuning.

This narrow range of gain margin and phase margin indicates that the control system for the Active magnetic bearings cannot tolerate an appreciable variation in the phase and gain of the return difference matrix $[G(s)H(s)]$ before its eigen value cross into the right-half s-plane. Though, GA-tuning has slightly improved the gain margin and phase margin compared to manually tuned LQG.

8 Conclusion

Active Magnetic bearings are very important mechatronic element of a machine. In this paper with some assumptions, the model of the AMB system is developed and it is shown that, the system is 2-input and 2-output MIMO system. State feedback controllers are designed for the AMB system. Before the controllers are designed the appropriate control loop was selected by the RGA analysis. From the RGA analysis it has been found that to control y_1 , u_1 should be manipulated and u_2 is manipulated to control y_2 .

Linear quadratic regulators (LQR) are designed by tuning the weighting matrices manually and using genetic algorithm (GA). The GA tuned LQR designed has managed to reduce the magnitude of the undesired undershoot almost by half and the overall performance is also as good as the manually tuned LQR.

LQG has better performance than LQR. As far as the tuning mechanisms are concerned in GA-tuned LQG the rise time and settling time are as good as the manually tuned LQG. In addition, the steady state error in GA-tuned LQG has a better value.

The genetic algorithm tuning has managed to improve the robustness of the manually tuned LQR. Although in the case of the LQG design, the manually tuned LQG has better robustness. Although, it has been observed that, the weighting matrices (Q and R) of the LQR design have small effect in improving the robustness of the LQG.

References

1. 6 Most Popular Types of Mechanical Bearings - Craftech Industries. Craftech Industries (2017). <http://www.craftechind.com/6-most-popular-types-of-mechanical-bearings/>, Accessed 01 Oct 2017
2. Bleuler, H.: A survey of magnetic levitation and magnetic bearing types. *JSME Int. J. Ser. III* **35**(3), 335–342 (1992)
3. Thrust Bearings Information | Engineering360. Globalspec.com (2017). http://www.globalspec.com/learnmore/mechanical_components/bearings_bushings/thrust_bearings, Accessed 05 Feb 2017
4. Schuhmann, T., Hofmann, W., Werner, R.: Improving operational performance of active magnetic bearings using kalman filter and state feedback control. *IEEE Trans. Ind. Electron.* **59**(2), 821–829 (2012)
5. Kuseyri, I.S.: Robust control and unbalance compensation of rotor/active magnetic bearing systems. *J. Vib. Control* **18**(6), 817–832 (2012)
6. Pesch, A.H., Sawicki, J.T.: Active magnetic bearing online levitation recovery through μ -synthesis robust control. In: *Multidisciplinary Digital Publishing Institute(MDPI) Actuators*, vol. 6, no. 2, pp. 1–14 (2017)
7. Pesch, A.H.; Hanawalt, S.P.; Sawicki, J.T.: A case study in control methods for active magnetic bearings. In: *Proceedings of the ASME Dynamic Systems and Control Conference*, San Antonio, TX, USA, pp. 22–24 (2014)
8. Schweitzer, G.: Active magnetic bearings - chances and limitations. In: *International Centre for Magnetic Bearings*, ETH Zurich, CH-8092 Zurich (2002)
9. Skogestad, S.: *Multivariable Feedback Control Analysis and Design*, 2nd edn. John Wiley & Sons, Hoboken (2001)

10. Michalewicz, Z., Janikow, C.: GENOCOP: a genetic algorithm for numerical optimization problems with linear constraints. *Commun. ACM* **39**(12), 175 (1996)
11. Doyle, J.: Guaranteed margins for LQG regulators. *IEEE Trans. Autom. Control* **23**(4), 756–757 (1978)
12. Tewari, A.: *Modern Control Design with MATLAB*, 1st edn. John Wiley & Sons, Hoboken (2002)
13. Hutterer, M., Hofer, M., Nenning, T., Schrödl, M.: LQG control of an active magnetic bearing with a special method to consider the gyroscopic effect. In: *ISMB14, 14th International Symposium on Magnetic Bearings*, Linz, Austria, 11–14 August 2014 (2014)
14. Schweitzer, G.: Applications and research topics for active magnetic bearings. In: *Proceedings IUTAM-Symposium on Emerging Trends in Rotor Dynamics*, Indian Institute of Technology, Delhi, India, 23–26 March 2009. Springer, Heidelberg (2011)